Bacterial defiance as a form of prodrug failure

Authors: Brandon Alexander Holt[1], Isabel Curro[1], and Gabriel A. Kwong[1–5,*]

Affiliations:

[1] Wallace H. Coulter Department of Biomedical Engineering, Georgia Tech College of - Engineering and Emory School of Medicine, Atlanta, GA 30332, USA; [2] Parker H. Petit Institute of Bioengineering and Bioscience, Atlanta, GA 30332, USA; [3] Institute for Electronics and Nanotechnology, Georgia Tech, Atlanta, GA 30332; [4] Integrated Cancer Research Center, Georgia Tech, Atlanta, GA, 30332; [5] Georgia ImmunoEngineering Consortium, Georgia Tech and Emory University, Atlanta, GA 30332.

[*]To whom correspondence should be addressed.

Address: 345 Ferst Dr, Atlanta, GA 30332

Phone: 404-385-3746

Email: gkwong@gatech.edu.

ABSTRACT

Classifying the mechanisms of antibiotic failure has led to the development of new treatment strategies for killing bacteria. Among the currently described mechanisms – which include resistance, persistence and tolerance – we propose defiance as a form of antibiotic failure specific to prodrugs. Using locked antimicrobial peptides (AMP) that are activated by bacterial proteases as a prototypic prodrug, we observe that although treatment eliminates bacteria across the vast majority of environmental conditions (e.g., temperature, concentration of growth nutrients), bacteria spontaneously switch from susceptibility to defiance under conditions that alter the competing rates between bacterial proliferation and prodrug activation. To identify the determinants of switch behavior, we model bacteria-prodrug dynamics as a multi-rate feedback system and identify a dimensionless quantity we call the Bacterial Advantage Heuristic (*BAH*) that perfectly classifies bacteria as either defiant or susceptible across a broad range of treatment conditions. By recognizing that the bacterial switch from susceptibility to defiance behaves analogously to electronic transistors, we construct prodrug logic gates (e.g., AND, OR, NOT, etc.) to allow assembly of an integrated 3-bit autonomous circuit that universally kills defiant bacteria under all possible combinations of *BAH* values (i.e., 000, 001, …, 111). Our study identifies a form of bacterial resistance specific to prodrugs that is described by a predictive dimensionless constant to reveal universal treatment strategies using prodrug biological circuits.

INTRODUCTION

The rise of multidrug-resistant bacteria coupled with the lack of newly developed antibiotics has created a serious public health threat [1, 2]. Understanding the causes of antibiotic failure improves the development of new drugs and informs clinical treatment strategies [3-5]. These failure mechanisms are broadly classified into three distinct categories (i.e., resistance, persistence, and tolerance), which are characterized by the change in drug concentration and exposure time required to kill bacteria [6]. For example, resistance is characterized by genetic mutations which result in bacteria requiring significantly higher concentrations of antibiotic (minimum inhibitory concentration, MIC) to be lethal. By contrast, bacteria exhibiting tolerance or persistence require increased drug exposure time (minimum duration for killing, MDK), with the latter exhibiting a biphasic killing profile (**Fig. 1A**). Further, bacteria populations become tolerant through environmental conditions or genetic mutations, whereas persistence is an actively maintained, non-heritable state exhibited by a subpopulation of bacteria. Discriminating between these survival strategies employed by bacteria is crucial for the development of new drugs and clinical treatment decisions [6].

Antibiotic success is markedly improved by proper drug titration, as overdosing leads to off-target toxicity and underdosing increases the likelihood of pathogens developing resistance[7, 8]. However, ideal drug doses are difficult to achieve over the course of treatment because infection burden changes dynamically over time, creating a moving target[7-9]. Prodrugs, which represent 10% of all FDA-approved drugs in the last decade, are a promising solution because they are automatically titrated by a disease-related activation mechanism and reduce the risk of off-target effects [10]. Prodrugs, such as ganciclovir [11] and sultamicillin [12], are administered as a biologically inactive form and are enzymatically or chemically activated by the diseased cells or pathogens. Here, we use prototypic auto-titrating prodrugs using cationic antimicrobial peptides (AMP), which evolved as a part of innate immunity and display broad-spectrum and prokaryote-specific

antimicrobial properties [13]. Cationic AMPs act by disrupting bacterial membranes and inducing inflammatory responses [14], but suffer from off-target toxicity and low stability *in vivo* [15, 16]. Our AMP prodrugs are activated directly by bacterial proteases, which are a major cause of virulence [17, 18] during infections and important targets for developing antibiotics [19]. Of these proteases, outer membrane protease T (OmpT), is a membrane-bound bacterial protein that is widely conserved across gram-negative bacteria of the *Enterobacteriaceae* family and recognizes a variety of targets that contribute to its virulence (e.g., plasminogen)[20-22]. In this work, we design cationic AMPs that are locked by charge complexation with anionic peptides and connected with a protease-cleavable linker substrate [23, 24] that is recognized by *E. coli* protease OmpT, such that increasing concentrations of bacteria yield higher concentrations of free drug.

While AMP prodrugs eliminate the majority of bacteria, we observe bacteria populations that we named "defiant", which proliferate in the presence of active drug by consistently outpacing prodrug activation at all stages of growth (i.e., log phase, stationary phase). To understand the mechanism by which bacteria become resistant to AMP prodrugs, we built a system of coupled ordinary differential equations (ODE) that model the dynamics of the bacteria-prodrug competition. We use this model to derive the dimensionless quantity – the Bacterial Advantage Heuristic (*B.A.H.*) – which predicts whether bacteria will become defiant under a broad range of conditions. At low *BAH* values, bacteria are susceptible to elimination, but after a critical threshold the bacteria switch to a state of defiance, in which the bacteria proliferate in the presence of activated drug. To combat this, we design biological circuits that universally treat all conditions (*BAH* values) by recognizing that AMP prodrugs behave analogously to transistors: above a critical *BAH* threshold (i.e., gate voltage), bacteria (i.e., input current) pass through the prodrug and exhibit defiance. We use this framework to build digital logic gates with prodrug transistors, which we use to construct a circuit that outputs 0 (i.e., dead bacteria) under all eight possible

combinations of three input *BAH* values. These quantitative mechanistic insights will better inform future drug design and treatment protocols leading to antibiotic success.

RESULTS & DISCUSSION

A bacteria-activatable prodrug targets *E. coli* protease OmpT

To construct bacteria-activated prodrugs, we synthesized cationic (polyarginine) antimicrobial peptides (AMP) in charge complexation with anionic peptide locks (polyglutamic acid) by a linker peptide (RRS|RRV) specific for the ubiquitous bacterial protease (OmpT)[23]. Upon proteolytic cleavage, AMP is unlocked to create a mechanism for auto-titration (**Fig. 1B**). To demonstrate specificity for OmpT, we synthesized an activity probe[21, 25-29] with free linker peptides containing a fluorescence-quencher pair and detected OmpT activity in samples incubated with recombinant OmpT or live *E. coli* culture. Conversely, we observed no activity in samples containing the serine protease inhibitor, Aprotinin, which inhibits OmpT when present in micromolar concentrations [20] (**Fig. 1C**). We observed similar cleavage activity using this linker substrate when fully integrated into AMP drug-lock complexes, confirming that linker presentation within a constrained conformational state did not affect cleavage activity (**Fig. 1D**). To measure cytotoxicity of unlocked drug, we dosed bacteria with free AMP and observed significant reduction in colonies compared to untreated controls (blue bar) (**Fig. 1E, F**). To confirm prodrug specificity, we synthesized AMP drug-lock complexes using linker peptides specific for OmpT or Tobacco Etch Virus Protease (TEV), which exhibits orthogonal protease specificity [30]. We observed elimination of bacteria only in samples containing OmpT-specific AMP prodrugs (black bars) or samples treated with both TEV and TEV-specific AMP prodrugs (red bars). All control samples containing either TEV-specific prodrug alone or Aprotinin inhibitor did not significantly reduce

bacteria load (**Fig. 1E, F, Table S1**). Our results showed that AMP drug-lock complexes are inert and lack cytotoxic activity until activation by protease activity.

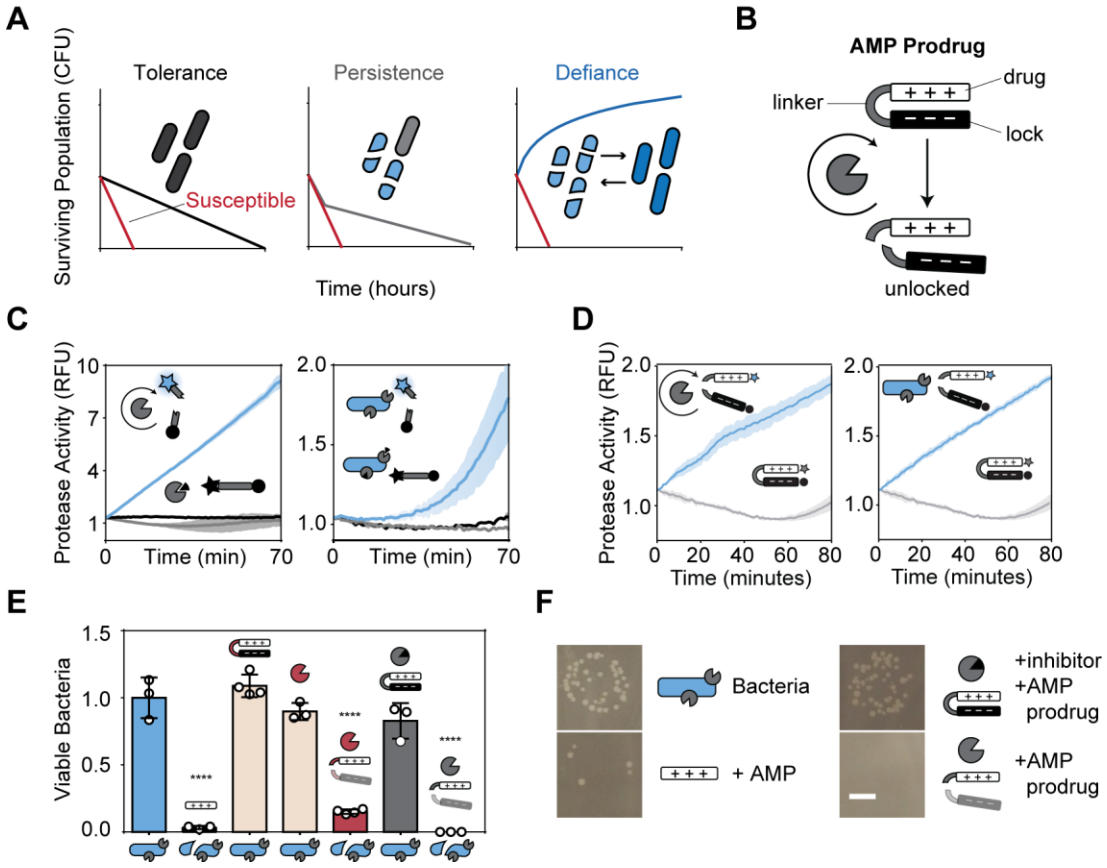

Figure 1. A bacteria-activatable prodrug targets *E. coli* protease OmpT (**A**) Schematic comparing time-dependent killing profiles of bacteria exhibiting tolerance, persistence, or defiance. Red line represents killing profile of susceptible bacteria. (**B**) A cationic AMP (RRRRRRRRR) locked by an anionic peptide (EEEEEEEEEEEEE) with a protease-cleavable linker (RRS|RRV) is activated by enzyme activity. (**C**) Cleavage assay measuring recombinant OmpT (grey protease) activity (left) and OmpT expressed on the surface of E. coli (right) against a fluorescence quenched peptide substrate (blue lines). Negative control is with the addition of inhibitor aprotinin (black triangle, black lines). Probe only control (grey lines). Shaded regions represent standard deviation (n = 3). (**D**) Cleavage assay measuring recombinant OmpT (left) and OmpT expressed by E. coli (right) against fluorescently labeled locked prodrug. Probe only control

(grey lines). Shading represents standard deviation (n = 3). All cleavage assays plotted as fold change in RFU from initial time point. (**E**) Bacteria viability assay quantifying drug toxicity relative to untreated bacteria control (blue bar). Positive control for AMP toxicity (black bar). Negative control for locked AMP or TEV protease alone (tan bars). Positive control for TEV protease with locked AMP (substrate: ENLYFQ|G, specific to TEV protease) (red bar). Negative control for locked AMP (substrate: RRSRRV, specific to OmpT) with OmpT inhibitor, aprotinin (grey bar). Experimental condition of bacteria treated with locked AMP activated by natively expressed OmpT (white bar). All values normalized and statistically compared to bacteria only control. Error bars represent standard deviation (n = 3). (**F**) Representative images of bacterial plates used to quantify viability with schematic legend (scale bar = 4 mm). * < 0.05, ** < 0.01, *** < 0.001, and **** < 0.0001.

Kinetic model of prodrug defiance reveals a binary outcome

To quantitatively understand how the rate of prodrug activation competes with the number of living bacteria, we built a mathematical model using a system of nonlinear ordinary differential equations (ODE). In our system, the three dynamic populations are the Bacteria, *B*, the Locked drug, *L*, and the Unlocked drug, *U*, for which we wrote governing ODEs where the time rate of change of each population as equal to the difference between the growth and decay functions. For this model, increased *E. coli* growth results in increased activation of the AMP, which in turn lyses bacteria, creating a negative feedback loop. Therefore, we modeled the bacteria population as positively influencing (i.e., green dashed arrows) the rate of enzymatic drug conversion (i.e., convert *L* to *U*) and the unlocked drug population as positively influencing the rate of bacterial death (**Fig 2A**). To account for the fact that bacterial growth rate, *r*, slows down as environmental resources become limiting (i.e., carrying capacity, B_{max}), we used a logistic growth model [31], which produces an S-shaped curve and has been used extensively in biology to study population

expansion[32] and tumor growth[33]. By contrast, the rate of *E. coli* death is proportional to the concentration of unlocked drug, *U*, according to a proportionality constant, *a*, that represents the amount of AMP required to kill *E. coli* per unit time (**Table S2, Equation 1.1**).

$$\frac{dB}{dt} = rB\left(1 - \frac{B}{B_{\max}}\right) - a^{-1}U \tag{1.1}$$

To model the rate of enzymatic activation of locked drugs, *L*, by OmpT, we used Michaelis-Menten kinetics [34], where the rate of substrate activation is determined by the catalytic rate of the reaction, k_{cat}, and the half-maximal substrate concentration, K_m (**Equation 1.2**). Our model assumes a well-mixed solution with free diffusion of substrate (i.e., locked drug), which is true for this study involving ~10^2 micromolar concentrations of AMP prodrug in an aqueous environment. Because the total amount of drug is conserved, we defined the activation rate of the unlocked drug, *U*, as the opposite of the degradation rate of the locked drug. In our system, AMPs kill *E. coli* through the perturbation of their membranes[35], so we assumed that once AMPs intercalate with bacterial membranes, they are unable to kill other bacteria and are thus removed from the system. We modeled the loss of AMPs according to a proportionality constant, a^*, that represents the number AMP required to kill one *E. coli* (**Equation 1.3**).

$$\frac{dL}{dt} = -k_{cat}B\frac{L}{K_m + L} \tag{1.2}$$

$$\frac{dU}{dt} = k_{cat}B\frac{L}{K_m + L} - a^* a^{-1}U \tag{1.3}$$

To fit this model to our system, we measured the relevant parameters, including enzymatic efficiency (e.g., k_{cat}, K_m), bacterial growth (e.g., r, B_{max}), and prodrug activity (e.g., a, a^*) (**Fig. S1, Table S2**). To experimentally validate our model across a broad range of parameter values, we tested nine conditions with different combinations of k_{cat} and r values, which we controlled with

ambient temperature, broth concentration and protease inhibitors (**Table S3**). Under these conditions over a 24-hour incubation with the prodrug, we quantified the number of living bacteria with serial CFU measurements, which closely matched the values predicted by our model (**Fig. 2B**). Interestingly, we observed a binary response to the prodrug, where bacteria were either susceptible to the prodrug and died or they showed a defiant phenotype and proliferated (**Fig. 3C**). These experiments demonstrate that when *E. coli* are exposed to the AMP prodrug, our model can be used to predict bacterial growth kinetics, which ultimately result in a binary outcome.

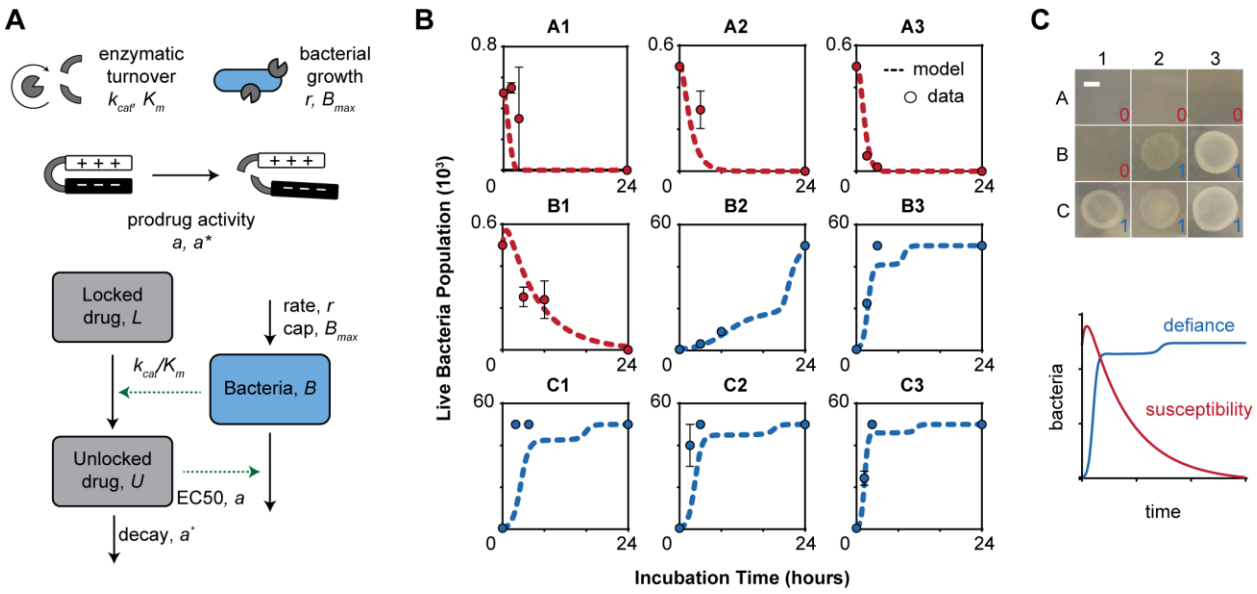

Figure 2. Kinetic model of prodrug defiance reveals a binary outcome. (**A**) Graphical representation of the model of bacteria and unlocked drug populations. Legend describes the agents associated with each variable. (**B**) Validating the model with serial CFU measurements (error bars SEM) and ODE model simulations of nine conditions given extracted growth rate and enzyme kinetics parameter values. (**C**) Agar plates showing presence/absence of bacterial growth and end-point for nine environmental conditions (A1—C3, scale bar = 4 mm). Schematic depicting that bacterial defiance is characterized by proliferation in the presence of activated drug.

Predicting bacterial defiance with a dimensionless constant

We demonstrated that bacteria exposed to a prodrug exhibit a binary outcome: susceptibility (i.e., death) or defiance (i.e., survival). Our model revealed that defiant bacteria populations exhibit a positive slope throughout the entire incubation, meaning the bacterial growth rate (e.g., r, B_{max}) is always greater than the enzyme-driven death rate (e.g., k_{cat}, K_m) (**Fig 3A**). This demonstrates how the balance between bacterial growth and enzymatic turnover determines whether *E. coli* will survive exposure to the prodrug. To derive a metric for these surviving bacteria (i.e., defiance), we used Buckingham Pi theorem to find a dimensionless quantity that represents the balance between growth rate and enzymatic turnover, which we defined as the Bacterial Advantage Heuristic (*B.A.H.*) (**Equation 1.4**).

$$B.A.H. = \log_{10}\left(\frac{r}{k_{cat}}\right) \tag{1.4}$$

This quantity reflects that bacteria have a higher probability of switching to the defiance phenotype under conditions that promote a faster growth rate, r, and slower enzymatic activity, k_{cat}. To predict the onset of the defiance phenotype, we sought to determine the critical *B.A.H.* value that distinguishes defiant bacteria from susceptible populations. Using our model, we simulated >2000 conditions with unique r, B_{max}, k_{cat}, and K_m values and compared the outcome with the *BAH* to find the critical value at which bacteria switch from susceptibility to defiance (BAH_{crit} ~ -11.37). To demonstrate that this critical value is independent from any system parameter, we individually fixed each of the four parameters (i.e., r, B_{max}, k_{cat}, and K_m) and calculated the resulting critical *BAH* value (**Fig 3B—E**). Additionally, the critical *BAH* was time-independent, as the value was the same across a range of incubation times (**Fig 3F—H**). To quantify the *BAH* for the nine experimental conditions, we conducted a series of experiments to measure the resulting k_{cat} and r values (**Fig S2**). We then used the computationally-derived critical *BAH* threshold to classify the phenotype of thirteen bacterial populations and perfectly predicted the onset of defiance (**Fig.**

3I—K AUROC = 1.00, n = 13). These results show that we can successfully treat defiant bacteria by changing the system parameters to decrease the *B.A.H.* below the critical threshold. To demonstrate this, we took a previously unsuccessful prodrug and decreased the *B.A.H.* by replacing the lock with a more efficient substrate sequence (i.e., higher k_{cat}), which allowed us to successfully treat the previously defiant population of bacteria (**Fig. S3**). These findings are important for the successful design and administration of prodrug therapies, which may be improved with small adjustments to fundamental pharmacokinetic parameters.

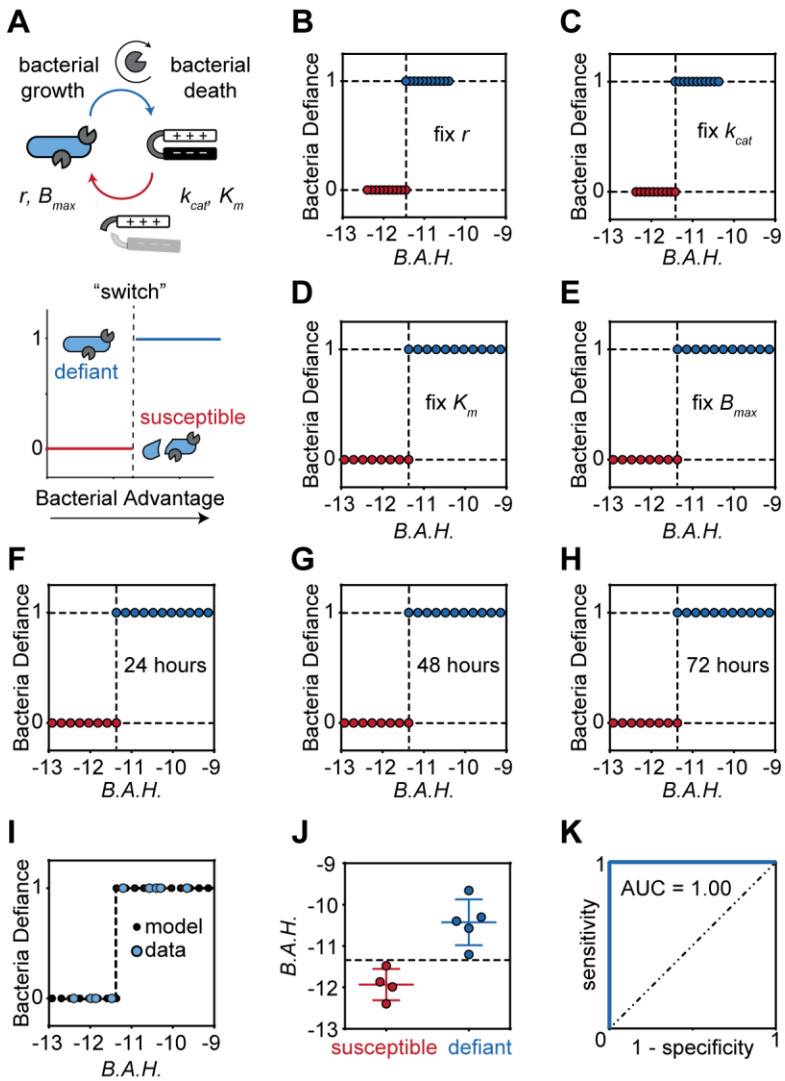

Figure 3. Predicting bacterial defiance with a dimensionless constant. (**A**) Schematic depicting the balance between bacteria growth and death, with the relevant parameters. Graph

shows the resulting "switch" like behavior that occurs at a critical *BAH* threshold. (**B—E**) Model simulations of outcome (bacterial defiance = 1, susceptibility = 0) vs. *BAH* value by controlling four parameters: r, k_{cat}, K_m, and B_{max}. In each panel, one of these four variables is fixed while the others are changing. (**F—H**) Model simulations of outcome vs. *BAH* value after increasing incubation times (e.g., 24, 48, 72 hours). (**I**) Correlating BAH with bacteria outcome to measure critical defiance value. (**J**) Grouping bacteria populations into defiant and susceptible based on *BAH*. (**K**) Using *BAH* to classify populations as defiant based on bacteria-driven parameters (r and k_{cat}/K_m).

Building biological transistors with prodrugs

We successfully treated defiant bacteria by changing just one aspect of the prodrug (i.e., the catalytic efficiency of the substrate) while all other system parameters were held constant. By contrast, treating bacteria under more dynamic, physiologically-relevant conditions requires prodrugs that work under multiple combinations of input variables (e.g., temperature, enzyme activity, etc.). We hypothesized that by making prodrugs that behave analogously to transistors, we could build biological circuits that process environmental signals and kill bacteria under a broad range of conditions. To accomplish this, we designed the complementary N-type and P-type transistors, which are used to construct all possible logic gates [36]. N-type transistors allow input current (I_{in}) to pass (I_{out}) when the gate signal (G) is *above* a defined threshold, whereas P-type transistors allow current to pass when the gate signal is *below* a defined threshold. We created N-type transistors with the AMP prodrug, which allowed input bacteria (B_{in}) to survive (B_{out}) when the *BAH* is above a critical value (**Fig. 4A**). To create P-type transistors, we used heat-triggered liposomes[37], which release their contents at temperatures above 37 ^{o}C (**Fig. S4**). At these temperatures, *E. coli* survive in the presence of a prodrug because they grow significantly faster[38], so we defined conditions above 37 ^{o}C as corresponding to *BAH* = 1 and below as *BAH*

= 0. By loading heat-triggered liposomes with ampicillin, a potent antibiotic for *E. coli* [39], we created a prodrug that kills bacteria (i.e., OUT = 0) when exposed to temperatures above 37 ºC (i.e., BAH = 1) (**Fig 4B**). These results demonstrate that two unique prodrugs can be used to build biological N-type and P-type transistors.

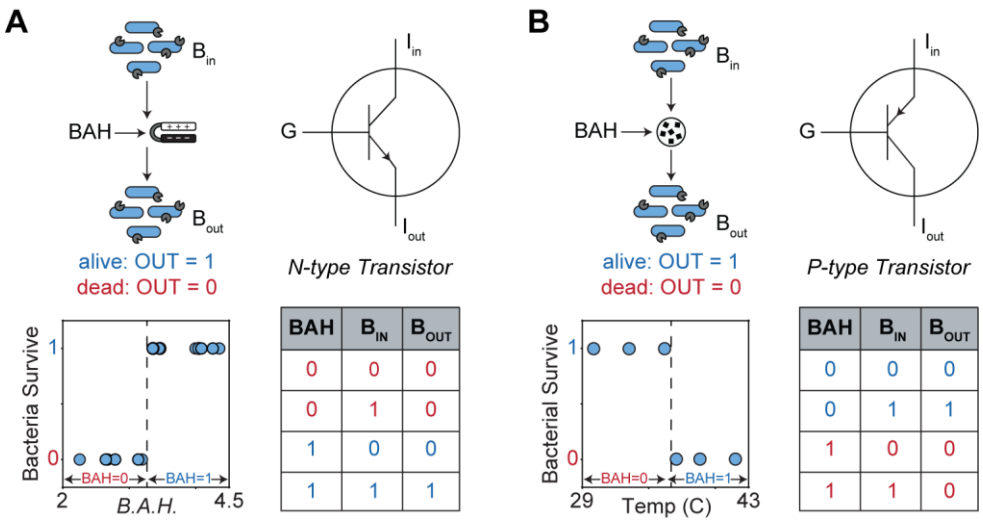

BAH	B_{IN}	B_{OUT}
0	0	0
0	1	0
1	0	0
1	1	1

BAH	B_{IN}	B_{OUT}
0	0	0
0	1	1
1	0	0
1	1	0

Figure 4. Building biological transistors with prodrugs (**A**) Schematic and truth table showing how the AMP prodrug behaves analogously to N-type transistors, in which the input signal (I_{in}, B_{in}) is allowed to pass when the gate signal (G, BAH) is *high*. (**B**) Schematic and truth table showing how the heat-triggered, drug loaded (black squares) liposomes (black circle) behaves analogously to P-type transistors, in which the input signal (I_{in}, B_{in}) is allowed to pass when the gate signal (G, BAH) is *low*. All truth tables depict ideal binary input-output combinations.

Combatting bacterial defiance with an autonomous, universal circuit

To demonstrate the advantage of using transistor-like prodrugs to combat defiance, we sought to design a biological circuit that universally kills bacteria under a set of changing environmental signals. To test multiple combinations of conditions, we chose three system variables (i.e., media,

temperature, substrate sequence), which independently influenced the bacteria-prodrug competition (i.e., BAH_A, BAH_B, BAH_C), to act as the circuit inputs. We designed a circuit to universally kill bacteria by computationally generating circuit layouts that output 0 (i.e., bacterial death) under all eight combinations of three inputs while using only AND, OR, and NOT gates (**Fig. 5A**). To create AND gates with prodrugs, we mirrored the arrangement of electronic transistors by placing two prodrugs (i.e., BAH_A *and* BAH_B) in series and sequentially dosing the bacteria. When exposed to all four possible inputs (i.e., 00, 01, 10, and 11), bacteria only survived the 11 condition (OUT = 1), which matched the ideal outputs of an AND gate (**Fig. 5B**). Whereas the AND comprised prodrugs in series, we built an OR gate by dosing two prodrugs in parallel (i.e., simultaneously). Using this circuit, bacteria survived in any case where at least one input *BAH* = 1, matching the ideal outputs of an OR gate (**Fig. 5C**). We created a NOT gate by using a P-type prodrug comprising ampicillin-loaded heat-triggered liposomes, which caused bacteria to die at high temperatures (i.e., *BAH* = 1) and survive at low temperatures (i.e., *BAH* = 0). (**Fig. 5D**). To validate the universal circuit, we incubated a combination of three AND gate prodrugs and one NOT gate prodrug with a population of bacteria under all eight environmental conditions. Whereas a single prodrug only eliminated bacteria in half of the input cases (**Fig. 5E**), our circuit autonomously eliminated bacteria under all eight combinations of the three environmental signals (**Fig. 5F**). These results demonstrate that by utilizing the transistor-like properties of prodrugs, we can design and administer biocircuits that combat bacterial defiance.

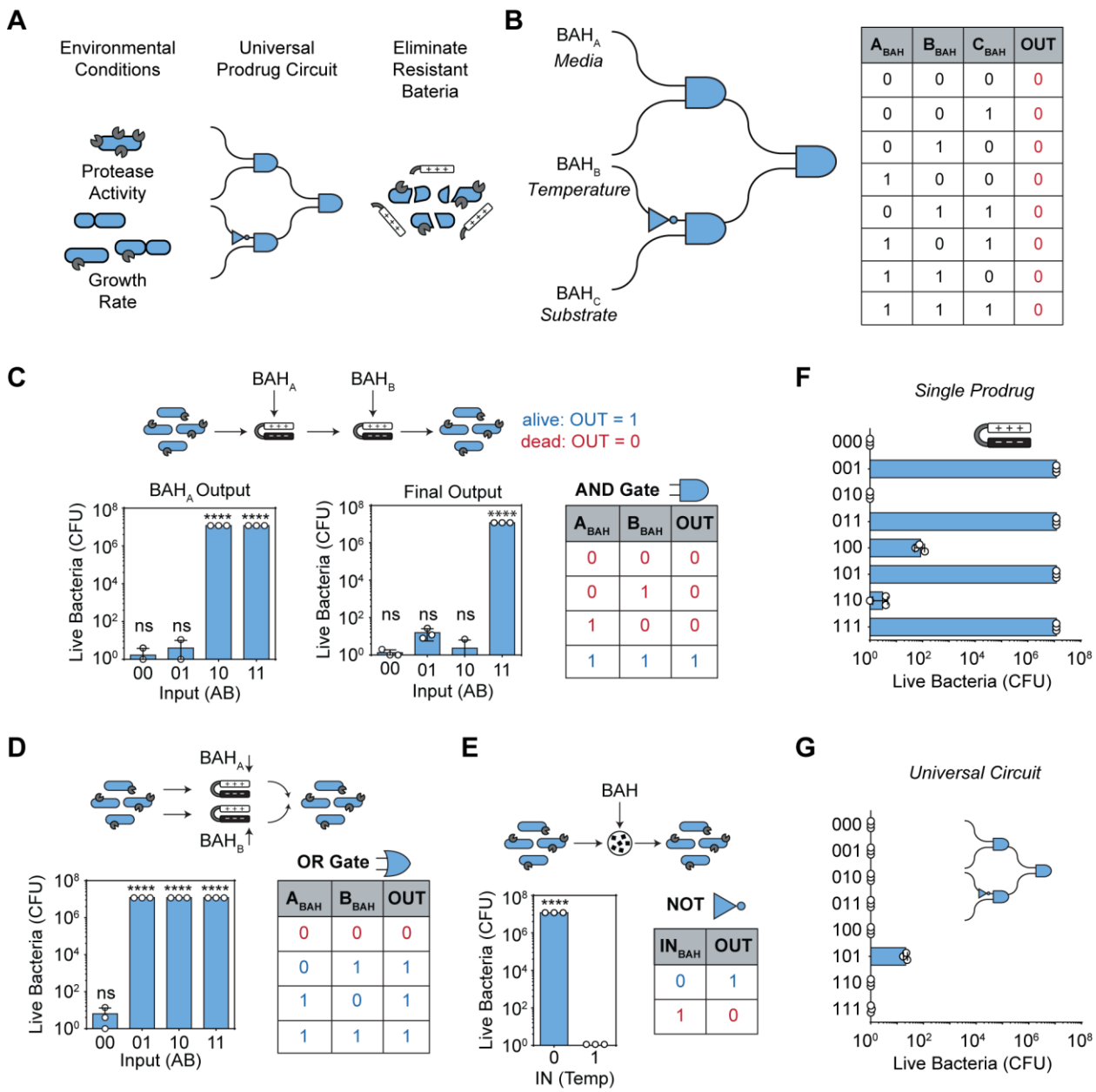

Figure 5. Combatting bacterial defiance with an autonomous, universal circuit. (**A**) Schematic depicting the concept of a universal prodrug circuit capable of treating defiant bacteria under a broad range of environmental conditions. (**B**) Logic circuit schematic depicting a function that universally outputs 0 for all possible combinations of three binary inputs. Truth table for universal circuit input-output combinations. (**C**) Bacterial viability assay validating the function of a prodrug-based AND gate. Schematic depicts two prodrug transistors arranged in series. (**D**)

Bacterial viability assay validating the function of a prodrug-based OR gate. Schematic depicts two prodrug transistors arranged in parallel. For AND and OR, input values were controlled with substrate sequence, where the substrate with high k_{cat}/K_m corresponds to *BAH* = 0 and the substrate with low k_{cat}/K_m corresponds to *BAH* = 1. (**E**) Bacterial viability assay validating the function of a prodrug-based NOT gate. Schematic depicts heat-triggered liposome (black circle) loaded with drug (black squares). BAH = 0 corresponds to temperature of 30 ^{o}C and BAH = 1 corresponds to 37 ^{o}C. (**F**) Bacterial viability assay quantifying the outcome of a single prodrug in the context of different environmental conditions. (**G**) Bacterial viability assay demonstrating the eight outputs of the autonomous circuit. All truth tables depict ideal binary input-output combinations. Error bars represent standard deviation (n = 3). * < 0.05, ** < 0.01, *** < 0.001, and **** < 0.0001.

CONCLUSION

The rising threat of antibiotic failure has motivated the classification of resistance mechanisms to improve the design of future treatment strategies. Currently studied classes of resistance (e.g., persistence, tolerance) classify bacteria based on killing curves or populational features (i.e., single cell, subpopulation, etc.). While previous studies have found that engineering prodrug substrates with higher affinity increased the probability of successful treatment [40, 41] and there are established genetic mutations that could potentially lead to defiance [42-44], there are no resistance phenotypes specific to prodrugs studied to date. Antimicrobial prodrugs, which are activated by bacterial activity, improve target specificity while introducing a unique element: the competition between bacterial growth and prodrug activation. In these studies, we establish the defiance phenotype as a form of antibiotic failure in which bacteria proliferate while activating prodrugs. To study bacterial defiance, we synthesized an AMP prodrug that was activated by bacterial protease activity and successfully killed *E. coli*. However, we found that this prodrug

failed in conditions where the bacteria grew faster than the rate at which they activated the drug. We developed a mathematical model of the bacteria-prodrug competition and derived a dimensionless constant (*B.A.H.*), which we used to perfectly predict the onset of the defiance phenotype in thirteen bacterial populations. These studies revealed that both environmental (e.g., temperature) and pharmacokinetic (e.g., half-life, substrate affinity) parameters can be engineered to improve prodrug therapies. To increase the success of prodrugs when multiple variables are affected, we constructed a universal biocircuit that processed three environmental signals to eliminate bacteria in all eight possible conditions. Taken together, this work establishes the defiance phenotype as a form of antibiotic failure specific to prodrugs and establishes a framework for engineering biological circuits capable of combatting defiance.

Author Contributions: G.A.K. and B.A.H conceived of the idea. G.A.K, B.A.H., and I.C. designed experiments and interpreted results, and wrote the manuscript. B.A.H. and I.C. carried out experiments.

Acknowledgments: This work was funded by an NIH Director's New Innovator Award (Award No. DP2HD091793). B.A.H is supported by the NSF GRFP, National Institutes of Health GT BioMAT Training Grant under Award Number 5T32EB006343 and the Georgia Tech President's Fellowship. This material is based upon work supported by the National Science Foundation Graduate Research Fellowship under Grant No. DGE-1650044 (B.A.H.). G.A.K. holds a Career Award at the Scientific Interface from the Burroughs Welcome Fund. The content is solely the responsibility of the authors and does not necessarily represent the official views of the National Institutes of Health. The authors would like to thank Ian Miller (Georgia Tech), Shreyas Dahotre (Georgia Tech), and Dr. Kyle Allison (Georgia Tech & Emory) for their helpful discussions.

EXPERIMENTAL PROCEDURES

Protease Cleavage Assays

All protease cleavage assays were performed with a BioTek Cytation 5 Imaging Plate Reader, taking fluorescent measurements at 485/528 nm (excitation/emission) for read-outs measuring peptide substrates terminated with FITC (Fluorescein isothiocyanate). Kinetic measurements were taken every minute over the course of 60 – 120 minutes at 37 C. Tobacco Etch Virus protease (TEVp), along with its substrate and buffer was obtained from Anaspec, Inc. (Fremont, CA). Activity RFU measurements were normalized to time 0 measurement, and as such represent fold change in signal. Outer Membrane Protease T (i.e., OmpT, Protease 7) was purchased from Lifespan Biosciences (Seattle, WA). OmpT fluorescent peptide substrate was custom ordered from Genscript (Piscataway, NJ).

Bacterial culture and cytotoxicity measurement

DH5α Escherichia coli were a gift from Todd Sulchek's BioMEMS lab at Georgia Tech. E. coli were cultured in LB broth (Lennox) at 37 C and plated on LB agar (Lennox) plates. LB broth was purchasd from Millipore Sigma (Burlington, MA) and LB agar was purchased from Invitrogen (Carlsbad, CA). AMP and locked AMP were custom ordered from Genscript (Piscataway, NJ). See Table S1 for more information. Bacteria were grown to a concentration of 10^9 CFU/mL before being used for experiments. Concentration was estimated by measuring the OD_{600} of the bacterial suspension, and assuming an OD_{600} of 1.000 corresponds to a concentration of 8×10^8 CFU/mL. Bacterial cell viability was measured by making eight 10-fold serial dilutions, and plating three 10 uL spots on an LB agar plate. Plates were incubated overnight at 37C, and CFUs were counted. Untreated bacteria CFU counts served as control for 0% cytotoxicity, and bacteria + IPA (or 0 countable CFUs) served as control for 100% cytotoxicity.

Liposome Preparation

DPPC and MPPC were purchased from Avanti Polar Lipics, inc. The heat-triggered NOT gate formulation was composed of DPPC:MPPC at the molar ratio 9:1, and were evaporated in cholorform to produce a lipid film. Films were rehydrated in 100% water containing 100 mg/mL ampicillin and were sonicated for 20 minutes. Lipid formulations were then purified using a PD-10 desalting column (GE Healthcare) and size was measured via dynamic light scattering (DLS, Malvern).

Computational model

The ODE modelling and solutions were performed in MATLAB 2016b. Code can be found in supplementary information.

Statistical Analysis

Statistical analysis was performed using statistical packages included in GraphPad Prism 6. To assess the significance of increase in signal due to protease cleavage, we used a two-way ANOVA (without repeated measures) followed by Sidak's multiple comparisons test. A one-way ANOVA followed by Dunnett's multiple comparisons test was used to compare experimental means to cells only control bacterial viability assays. Two-way ANOVA followed by Sidak's multiple comparisons test used to compare experimental means to control for bacterial cytotoxicity at multiple starting concentrations.

SUPPLEMENTARY INFORMATION, FIGURES, AND TABLES

Measuring kinetic parameters for the ODE model

To measure drug cytotoxicity, we quantified the percent of viable bacteria when exposed to unlocked AMP drug doses ranging from nanomolar to millimolar concentrations and observed a spike in cytotoxicity in the micromolar range (**Fig. S1A**). To calculate bacterial growth rate constants, we incubated bacteria in broth or water at 37C and measured OD_{600} over the course of 8 hours, revealing a higher growth rate in broth consistent with published values[31, 44] (3.0 > 0.1 h^{-1}) (**Fig. S1B**). To quantify enzymatic velocity, we measured proteolytic velocity (moles L^{-1} s^{-1}) under substrate concentrations ranging from 0—200 uM and fit the Michaelis-Menten equations to this data to calculate k_{cat} and K_m (**Fig. S1C**). Using these measured parameters (**Table S2**), we generated kinetic curves for bacteria number and drug concentration over time. The model showed that after a period of initial bacterial growth, the lagging drug population eliminated the infection burden. While the initial reservoir of locked drug concentration was ~200 µM, the unlocked drug never rose above 5 µM (**Fig. S1D**), revealing that this system maintains the minimal drug concentration required to kill the infection.

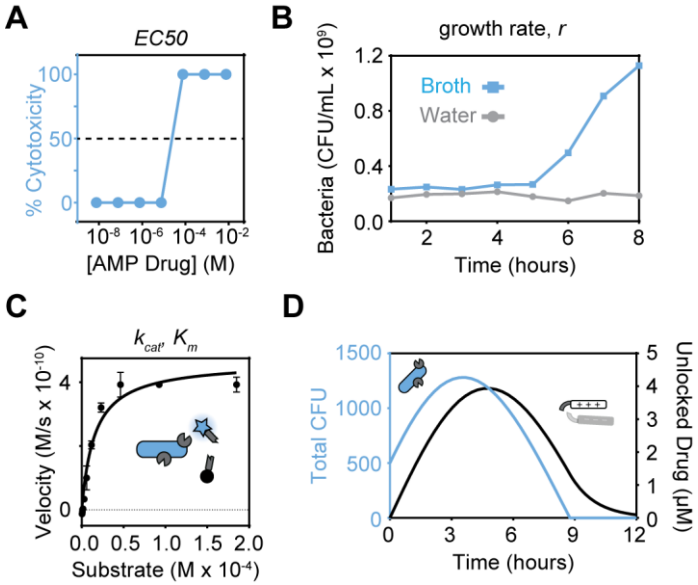

Fig. S1. Measuring kinetic parameters for the ODE model. (**A**) EC50 measurement on a sample of *E. coli* exposed to increasing concentrations of AMP. (**B**) Growth rate calculation of *E. Coli* in broth and water by measuring OD at 600 nm. (**C**) Measuring k_{cat}/K_m from a series of cleavage assays incubating *E. coli* at a range of substrate concentrations. (**D**) Predicting the dynamics of the bacteria and unlocked drug population given empirical parameter values. Error bars are standard deviation (n = 3).

Estimating bacterial growth rate and enzymatic activity with parameter fitting

To estimate bacterial growth rate (r) and enzymatic efficiency (k_{cat}, K_m), we used parameter fitting methods to a simplified model without a prodrug (**Fig. S3**). In this model, the prodrug is substituted with a fluorescent probe (P), which is activated with the same substrate sequence as the AMP prodrug. To simplify the model, we defined one bacterium, with ~ 2.5×10^3 OmpT proteases per cell [45], as equivalent to one effective enzyme. The concentration of cleaved fluorescent probe is monitored over time, and the bacterial concentration is quantified at serial time points. We fit this data to the two equations modelling bacterial growth and activation of the fluorescent probe (**Equations S1.1, S1.2**).

$$\frac{dB}{dt} = rB\left(1 - \frac{B}{B_{\max}}\right) \tag{S1.1}$$

$$\frac{dP}{dt} = -k_{cat} B \frac{P}{K_m + P} \tag{S1.2}$$

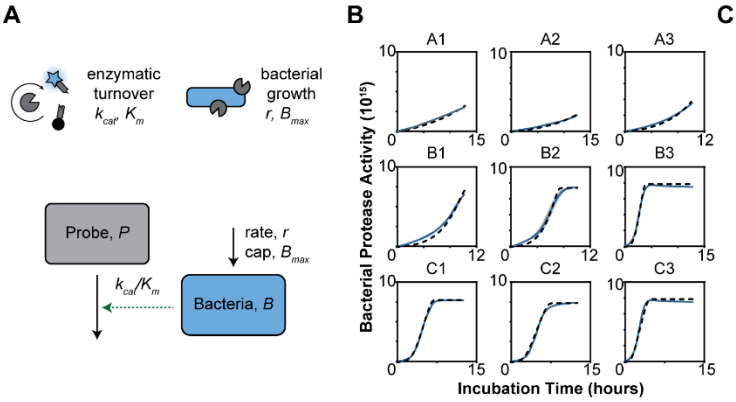

C

Condition	Temperature	LB Broth Concentration	$r(h^{-1})$	$k_{cat}(h^{-1}) \times 10^{10}$	B.A.H.
A1	37C	0%	0.1	25	-12.3979
A2	30C	2%	0.14	13.6	-11.9874
A3	37C	2%	0.3	22	-11.8653
B1	37C	4%	0.5	15	-11.4771
B2	37C	6%	0.85	13.6	-11.2041
B3	37C	20%	2.2	1	-9.65758
C1	30C	20%	1.4	5.2	-10.5699
C2	30C	66%	1.6	4	-10.3979
C3	37C	66%	3	6	-10.301

Fig. S2. Estimating bacterial growth rate and enzymatic activity with parameter fitting. (**A**) Schematic of model used to quantify r and k_{cat} from bacterial cleavage assays. (**B**) Bacterial cleavage assays (blue line), from which growth rate (r) and enzyme kinetics (k_{cat}/K_m) are extracted, and *BAH* is calculated (inset). Dotted line represents model after parameter fitting. (**C**) Table of r and k_{cat} values quantified from model in each condition with varying temperature and LB broth concentration.

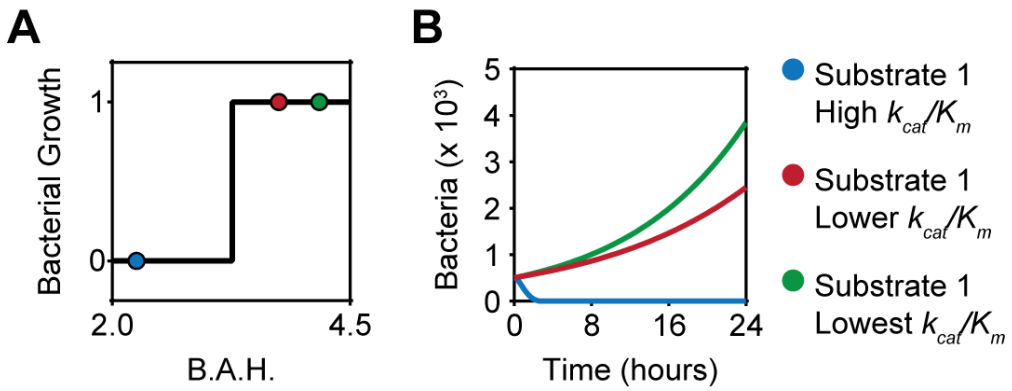

Fig. S3. Altering drug efficacy with substrate affinity. (**A**) Bacteria viability assay post 24 hour incubation with drug unlocked by various substrates. Bacterial growth = 1 if colonies were present after plating, and bacterial growth = 0 if there were no colonies present (n = 3). B.A.H. values extrapolated from bacteria + probe velocity measurements fitted to model. (**B**) Bacteria dynamics predicted by model given three different enzyme kinetics.

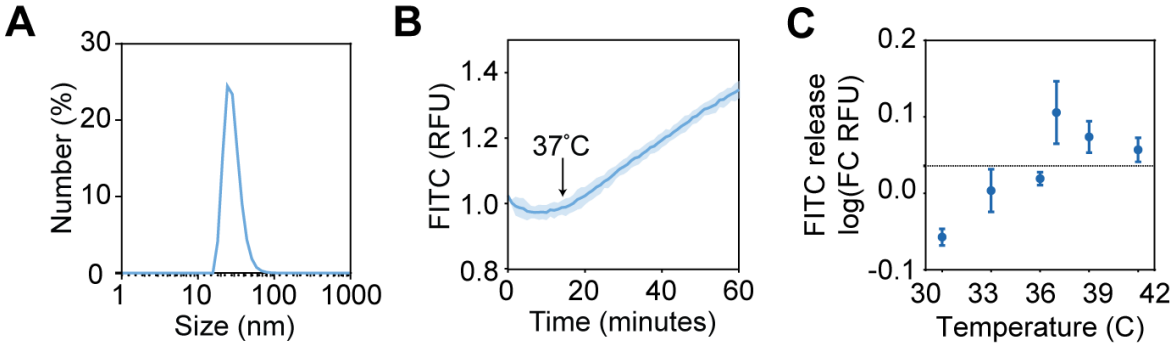

Fig. S4. Validating heat-triggered liposomes. (**A**) Dynamic light scattering of liposome formulation to determine particle size (~35 nm). Histogram is plotted as the mean of independent measurements (n = 3). (**B**) Fluorescent assay measuring the heat-triggered release of liposome contents. Liposomes were loaded with 100 mM FITC, and heated from 25 C to 37C (indicated by arrow). Lines are plotted as means of independent measurements, shading represents standard deviation (n = 3). (**C**) Fluorescent assay measuring the release of FITC from heat triggered liposomes at various temperatures. All samples were heated to 30 C for 10 minutes, then heated at the plotted temperature for 30 minutes. Measurements are plotted as fold change in RFU between final measurement and measurement at 30 C. Error bars represent standard deviation (n = 3).

TABLE S1

Name	Peptide Sequence
Locked AMP (substrate 1)	EEEEEEEEEEEEERRSRRVRRRRRRRRR
Locked AMP (substrate 2)	EEEEEEEEEEERKTRRRRRRRRR
Locked AMP (substrate 3)	EEEEEEEEENLYFQGRRRRRRRRRR
Locked AMP Probe	DABCYL-EEEEEEEEEEEEERRSRRVRRRRRRRRR[Lys(5-FAM)]
OmpT Probe	DABCYL-RRSRRV-Lys(5-FAM)

TABLE S2

Variable	Value	Units	Notes
r	0.1—3	h^{-1}	Bacterial growth rate
kcat	0.7—25e10	h^{-1}	Enzyme catalytic turnover
Km	9e12	μL^{-1}	Michaelis constant
Bmax	1000	μL^{-1}	Max bacteria concentration in tube
a	1e11	h^{-1}, AMP/bacteria/hr	Cytotoxic efficiency, EC50
a^*	2.4e11	AMP/bacteria	AMP decay

TABLE S3

Location (row, column)	Temperature	LB Broth Concentration	***r*** **(h^{-1})**	k_{cat} **(h^{-1}) x 10^{10}**
A1	37C	0%	0.1	25
A2	30C	2%	0.14	13.6
A3	37C	2%	0.3	22
B1	37C	4%	0.5	15
B2	37C	6%	0.85	13.6
B3	37C	20%	2.2	1
C1	30C	20%	1.4	5.2
C2	30C	66%	1.6	4
C3	37C	66%	3	6

REFERENCES

1. Baquero, F., Martinez, J.L. & Canton, R. Antibiotics and antibiotic resistance in water environments. *Current opinion in biotechnology* **19**, 260-265 (2008).
2. Gullberg, E. et al. Selection of Resistant Bacteria at Very Low Antibiotic Concentrations. *PLOS Pathogens* **7**, e1002158 (2011).
3. Molina-Quiroz, R.C. et al. Cyclic AMP Regulates Bacterial Persistence through Repression of the Oxidative Stress Response and SOS-Dependent DNA Repair in Uropathogenic Escherichia coli. *mBio* **9** (2018).
4. Cohen, N.R., Lobritz, M.A. & Collins, J.J. Microbial persistence and the road to drug resistance. *Cell host & microbe* **13**, 632-642 (2013).
5. Allison, K.R., Brynildsen, M.P. & Collins, J.J. Metabolite-enabled eradication of bacterial persisters by aminoglycosides. *Nature* **473**, 216 (2011).
6. Brauner, A., Fridman, O., Gefen, O. & Balaban, N.Q. Distinguishing between resistance, tolerance and persistence to antibiotic treatment. *Nature Reviews Microbiology* **14**, 320 (2016).
7. Bielicki, J.A. et al. Not too little, not too much: problems of selecting oral antibiotic dose for children. *BMJ : British Medical Journal* **351** (2015).
8. Bailey, A.M., Stephan, M., Weant, K.A. & Justice, S.B. Dosing of Appropriate Antibiotics and Time to Administration of First Doses in the Pediatric Emergency Department. *The journal of pediatric pharmacology and therapeutics : JPPT : the official journal of PPAG* **20**, 309-315 (2015).
9. Iizumi, T., Battaglia, T., Ruiz, V. & Perez Perez, G.I. Gut Microbiome and Antibiotics. *Archives of medical research* **48**, 727-734 (2017).
10. Rautio, J., Meanwell, N.A., Di, L. & Hageman, M.J. The expanding role of prodrugs in contemporary drug design and development. *Nature Reviews Drug Discovery* **17**, 559 (2018).
11. Al-Badr, A.A. & Ajarim, T.D.S. in Profiles of Drug Substances, Excipients and Related Methodology, Vol. 43. (ed. H.G. Brittain) 1-208 (Academic Press, 2018).
12. Baltzer, B. et al. Mutual pro-drugs of beta-lactam antibiotics and beta-lactamase inhibitors. *J Antibiot (Tokyo)* **33**, 1183-1192 (1980).
13. Zhang, L.-j. & Gallo, R.L. Antimicrobial peptides. *Current Biology* **26**, R14-R19 (2016).
14. Mahlapuu, M., Håkansson, J., Ringstad, L. & Björn, C. Antimicrobial Peptides: An Emerging Category of Therapeutic Agents. *Frontiers in Cellular and Infection Microbiology* **6** (2016).
15. Wimley, W.C. & Hristova, K. Antimicrobial Peptides: Successes, Challenges and Unanswered Questions. **239**, 27-34 (2011).
16. Bradshaw, J. Cationic antimicrobial peptides : issues for potential clinical use. *BioDrugs : clinical immunotherapeutics, biopharmaceuticals and gene therapy* **17**, 233-240 (2003).
17. Frees, D., Brondsted, L. & Ingmer, H. Bacterial proteases and virulence. *Sub-cellular biochemistry* **66**, 161-192 (2013).
18. Ingmer, H. & Brondsted, L. Proteases in bacterial pathogenesis. *Research in microbiology* **160**, 704-710 (2009).
19. Culp, E. & Wright, G.D. Bacterial proteases, untapped antimicrobial drug targets. *The Journal Of Antibiotics* **70**, 366 (2016).
20. Brannon, J.R. et al. Inhibition of outer membrane proteases of the omptin family by aprotinin. *Infection and immunity* **83**, 2300-2311 (2015).
21. McCarter, J.D. et al. Substrate Specificity of the Escherichia coli Outer Membrane Protease OmpT. *Journal of Bacteriology* **186**, 5919-5925 (2004).
22. Grodberg, J. & Dunn, J.J. ompT encodes the Escherichia coli outer membrane protease that cleaves T7 RNA polymerase during purification. *Journal of Bacteriology* **170**, 1245-1253 (1988).

23. Olson, E.S. et al. In vivo characterization of activatable cell penetrating peptides for targeting protease activity in cancer. *Integrative biology : quantitative biosciences from nano to macro* **1**, 382-393 (2009).
24. Franzman, M.R. et al. Targeted antimicrobial activity of a specific IgG-SMAP28 conjugate against Porphyromonas gingivalis in a mixed culture. *International journal of antimicrobial agents* **33**, 14-20 (2009).
25. Kwong, G.A. et al. Mass-encoded synthetic biomarkers for multiplexed urinary monitoring of disease. *Nat Biotech* **31**, 63-70 (2013).
26. Holt, B.A., Mac, Q.D. & Kwong, G.A. Nanosensors to Detect Protease Activity In Vivo for Noninvasive Diagnostics. *JoVE*, e57937 (2018).
27. Mac, Q.D. et al. Non-invasive early detection of acute transplant rejection via nanosensors of granzyme B activity. *Nature biomedical engineering* (2019).
28. Zhuang, Q., Holt, B.A., Kwong, G.A. & Qiu, P. Deconvolving multiplexed protease signatures with substrate reduction and activity clustering. *bioRxiv*, 564906 (2019).
29. Holt, B.A. et al. Fc microparticles can modulate the physical extent and magnitude of complement activity. *Biomaterials science* **5**, 463-474 (2017).
30. Kapust, R.B. et al. Tobacco etch virus protease: mechanism of autolysis and rational design of stable mutants with wild-type catalytic proficiency. *Protein Engineering, Design and Selection* **14**, 993-1000 (2001).
31. Fujikawa, H., Kai, A. & Morozumi, S. A new logistic model for bacterial growth. *Shokuhin eiseigaku zasshi. Journal of the Food Hygienic Society of Japan* **44**, 155-160 (2003).
32. Verhulst, P.-F. Mathematical Researches into the Law of Population Growth Increase. *Nouveaux Mémoires de l'Académie Royale des Sciences et Belles-Lettres de Bruxelles.* (1845).
33. Atuegwu, N.C. et al. Parameterizing the Logistic Model of Tumor Growth by DW-MRI and DCE-MRI Data to Predict Treatment Response and Changes in Breast Cancer Cellularity during Neoadjuvant Chemotherapy. *Translational Oncology* **6**, 256-264 (2013).
34. Menten, L. & Michaelis, M. Die kinetik der invertinwirkung. *Biochem Z* **49**, 333-369 (1913).
35. Roversi, D. et al. How Many Antimicrobial Peptide Molecules Kill a Bacterium? The Case of PMAP-23. *ACS Chemical Biology* **9**, 2003-2007 (2014).
36. Amos, S.W. & James, M. Principles of Transistor Circuits. (2000).
37. Needham, D., Anyarambhatla, G., Kong, G. & Dewhirst, M.W. A new temperature-sensitive liposome for use with mild hyperthermia: characterization and testing in a human tumor xenograft model. *Cancer research* **60**, 1197-1201 (2000).
38. Farewell, A. & Neidhardt, F.C. Effect of Temperature on In Vivo Protein Synthetic Capacity in Escherichia coli. *Journal of Bacteriology* **180**, 4704-4710 (1998).
39. Thonus, I.P., Fontijne, P. & Michel, M.F. Ampicillin susceptibility and ampicillin-induced killing rate of Escherichia coli. *Antimicrobial agents and chemotherapy* **22**, 386-390 (1982).
40. Barak, Y. et al. New enzyme for reductive cancer chemotherapy, YieF, and its improvement by directed evolution. *Molecular cancer therapeutics* **5**, 97-103 (2006).
41. Jordan, A.M., Khan, T.H., Osborn, H.M., Photiou, A. & Riley, P.A. Melanocyte-directed enzyme prodrug therapy (MDEPT): development of a targeted treatment for malignant melanoma. *Bioorganic & medicinal chemistry* **7**, 1775-1780 (1999).
42. Kramer, R.A., Zandwijken, D., Egmond, M.R. & Dekker, N. In vitro folding, purification and characterization of Escherichia coli outer membrane protease ompT. *European journal of biochemistry* **267**, 885-893 (2000).
43. Kramer, R.A. et al. Identification of essential acidic residues of outer membrane protease OmpT supports a novel active site. *FEBS letters* **505**, 426-430 (2001).

44. Jin, D.J., Cagliero, C. & Zhou, Y.N. Growth rate regulation in Escherichia coli. *FEMS microbiology reviews* **36**, 269-287 (2012).
45. Ishihama, Y. et al. Protein abundance profiling of the Escherichia coli cytosol. *BMC Genomics* **9**, 102 (2008).

5